Four-dimensional parameter estimation of plane waves using swarming intelligence

Fawad Zaman[a)†], Ijaz Mansoor Qureshi[b)‡], Fahad Munir[a)§], and Zafar Ullah Khan[a)¶]

[a)] *Department of Electronic Engineering, Faculty of Engineering and Technology International Islamic University Sector H-10, Islamabad, Pakistan*

[b)] *Department of Electrical Engineering, Air University, Islamabad, Pakistan*

(Received 4 September 2013; revised manuscript received 16 January 2014; published online 22 May 2014)

This paper proposes an efficient approach for four-dimensional (4D) parameter estimation of plane waves impinging on a 2-L shape array. The 4D parameters include amplitude, frequency and the two-dimensional (2D) direction of arrival, namely, azimuth and elevation angles. The proposed approach is based on memetic computation, in which the global optimizer, particle swarm optimization is hybridized with a rapid local search technique, pattern search. For this purpose, a new multi-objective fitness function is used. This fitness function is the combination of mean square error and the correlation between the normalized desired and estimated vectors. The proposed hybrid scheme is not only compared with individual performances of particle swarm optimization and pattern search, but also with the performance of the hybrid genetic algorithm and that of the traditional approach. A large number of Monte–Carlo simulations are carried out to validate the performance of the proposed scheme. It gives promising results in terms of estimation accuracy, convergence rate, proximity effect and robustness against noise.

Keywords: amplitude estimation, direction of arrival estimation, frequency estimation, genetic algorithm

PACS: 84.40.Ba, 84.40.Xb, 07.05.Mh, 33.20.Bx **DOI:** 10.1088/1674-1056/23/7/078402

1. Introduction

Parameter estimation of plane waves has been a hot area of research for the last few decades. It has applications in the field of radar, sonar, radio astronomy, mobile communication, etc.[1–4] The main parameters of plane waves which we need to estimate at sensor arrays are frequency, amplitude, elevation and azimuth angles. The most common problems encountered during the estimation of these parameters are the estimation failure, pair matching and computational complexity. Researchers have used different techniques along with different geometries of sensor array e.g., linear arrays,[5,6] planar array,[7,8] parallel shape array[9] and L-shaped arrays (1-L & 2-L shaped arrays)[10,11] to mitigate the problem, but they have one or the other of the above-mentioned problems.

In Ref. [12], an efficient approach based on the genetic algorithm hybridized with pattern search (GA-PS) was proposed, that used mean square error (MSE) as a fitness evaluation function. The proposed algorithm in Ref. [12], automatically paired the unknown parameters, produced better estimation accuracy and had less computational cost as compared to the existing traditional techniques.[11] The performance of Ref. [12] can be made even better if we use a new multi-objective fitness function.

In this paper, we have used particle swarm optimization (PSO) as a global optimizer hybridized with a local optimizer, pattern search (PSO-PS). This estimates not only the three-parameters i.e., amplitude, elevation and azimuth angles of the sources as in Ref. [12] but also their frequencies. Moreover, it uses a multi-objective fitness function which is a combination of MSE and the correlation between the normalized desired and estimated vectors. It is not only compared with PSO and PS, but also with that of another hybrid technique (GA-PS).[12] We have also compared the results of our proposed scheme with a non-heuristic traditional technique[13] where frequency has also been calculated. The simulation results verify that the PSO-PS has better performance in terms of convergence rate, estimation accuracy, proximity effect and robustness against noise.

The remaining paper is structured as follows. In Section 2, the data model is discussed, while Section 3 carries the proposed methodology's structure. In Section 4, the proposed scheme is compared with PSO, PS and GA-PS. In Section 5, we have compared our results with some traditional techniques, while Section 6 summarizes the paper and suggests some future work directions.

2. Data model

In this section, we have developed a data model for M narrow band sources existing in the Fraunhofer zone (far field). For this purpose, we have considered a 2-L shaped sensor ar-

†Corresponding author. E-mail: fawad.phdee31@iiu.edu.pk
‡Corresponding author. E-mail: imqureshi@mail.au.edu.pk
§Corresponding author. E-mail: fahad.phdee57@iiu.edu.pk
¶Corresponding author. E-mail: zafarullah.phdee13@iiu.edu.pk

© 2014 Chinese Physical Society and IOP Publishing Ltd

ray that has already shown better performance than a linear array,[5,6] a planar array,[7,8] a parallel shaped array[9] and a 1-L shaped array.[10] This array consists of 3-ULA placed along the x axis, y axis and z axis. Each ULA is composed of $Q-1$ sensors while the reference sensor is common for all of them as shown in Fig. 1.

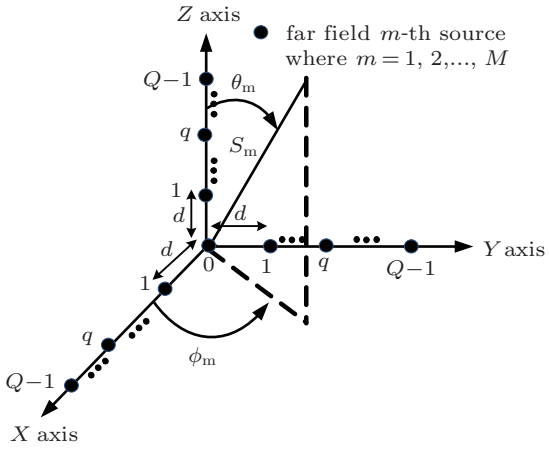


Fig. 1. Configuration of 2-L shaped array.

For $M < Q$, the response of the q-th sensor placed in the z axis sub-array can be represented as

$$y_{zq} = \sum_{m=1}^{M} s_m b_z(f_m, \theta_m) + n_{zq}, \tag{1}$$

where

$$b_z(f_m, \theta_m) = \exp(-\mathrm{j} q k_m d \cos\theta_m), \quad 0 \le q \le Q-1, \tag{2}$$

where d is separation between any two adjacent sensors in the array and can be given as

$$d = \lambda_{\min}/2, \tag{3}$$

where $\lambda_{\min} = c/f_{\max}$, c is the speed of light and $f_{\max}$ represents the maximum frequency expected from the sources. Besides, in Eq. (2), k_m is the wave number of the m-th source, given by

$$k_m = 2\pi/\lambda_m, \tag{4}$$

where $\lambda_m = c/f_m$, f_m is the frequency of the m-th source. By using Eqs. (2)–(4) in Eq. (1), we obtain

$$y_{zq} = \sum_{m=1}^{M} s_m \exp\left[-\mathrm{j}\frac{f_m}{f_{\max}}(q\pi\cos\theta_m)\right] + n_{zq}. \tag{5}$$

In vector form, equation (5) can be given as

$$\boldsymbol{y}_z = \boldsymbol{B}_z(f, \theta)\boldsymbol{s} + \boldsymbol{n}_z, \tag{6}$$

where $\boldsymbol{B}_z$ is a steering matrix which contains the frequencies and elevation angles of M sources received on a z axis sub-array, i.e.,

$$\boldsymbol{B}_z(f, \theta) = [\boldsymbol{b}_z(f_1, \theta_1), \boldsymbol{b}_z(f_2, \theta_2), \ldots, \boldsymbol{b}_z(f_m, \theta_m), \ldots, \boldsymbol{b}_z(f_M, \theta_M)]. \tag{7}$$

Similarly, $\boldsymbol{s}$ contains the sources amplitudes and can be given as

$$\boldsymbol{s} = [s_1, s_2, \ldots, s_m, \ldots, s_M]^{\mathrm{T}}. \tag{8}$$

The response of the q-th sensor in the sub-array along the x axis for M sources, can be given as

$$y_{xq} = \sum_{m=1}^{M} s_m b_x(f_m, \theta_m, \phi_m) + n_{xq}, \tag{9}$$

$$b_x(f_m, \theta_m, \phi_m) = \exp(-\mathrm{j} q k_m d \sin\theta_m \cos\phi_m). \tag{10}$$

Therefore, equation (9) can be represented as

$$y_{xq} = \sum_{m=1}^{M} s_m \exp\left[-\mathrm{j}\frac{f_m}{f_{\max}}(q\pi\sin\theta_m\cos\phi_m)\right] + n_{xq}. \tag{11}$$

In vector form, equation (11) can be given as

$$\boldsymbol{y}_x = \boldsymbol{B}_x(f, \theta, \phi)\boldsymbol{s} + \boldsymbol{n}_x, \tag{12}$$

where $\boldsymbol{B}_x$ is the steering matrix which contains the frequencies, elevation and azimuth angles of M sources received on the x axis sub-array and can be written as

$$\boldsymbol{B}_x(f, \theta, \phi) = [\boldsymbol{b}_x(f_1, \theta_1, \phi_1), \boldsymbol{b}_x(f_2, \theta_2, \phi_2), \ldots, \boldsymbol{b}_x(f_m, \theta_m, \phi_m), \ldots, \boldsymbol{b}_x(f_M, \theta_M, \phi_M)]. \tag{13}$$

Similarly, the response of the q-th sensor in the sub-array along the y axis for M sources can be given as

$$y_{yq} = \sum_{m=1}^{M} s_m b_x(f_m, \theta_m, \phi_m) + n_{yq}, \tag{14}$$

$$b_y(f_m, \theta_m, \phi_m) = \exp(-\mathrm{j} q k_m d \sin\theta_m \sin\phi_m). \tag{15}$$

In simplified form Eq. (14) can be given as

$$y_{yq} = \sum_{m=1}^{M} s_m \exp\left[-\mathrm{j}\frac{f_m}{f_{\max}}(q\pi\sin\theta_m\sin\phi_m)\right] + n_{yq}. \tag{16}$$

In vector form, it can be given as

$$\boldsymbol{y}_y = \boldsymbol{B}_y(f, \theta, \phi)\boldsymbol{s} + \boldsymbol{n}_y. \tag{17}$$

In Eqs. (6), (12), and (17), $\boldsymbol{n}_z$, $\boldsymbol{n}_x$, $\boldsymbol{n}_y$ are additive white Gaussian noise (AWGN) vectors are added at the output of each sensor in the respective sub-array and can be defined as

$$\boldsymbol{n}_w = [n_{w1}, n_{w2}, \ldots, n_{wQ}]^{\mathrm{T}}, \tag{18}$$

where $w = x, y, z$. The noise has zero mean and unit variance. They are iid and independent of source signals. From Eqs. (5), (11) and (16), it is obvious that the unknown parameters are the amplitudes (s_m), frequencies (f_m), elevation angles (θ_m), and azimuth angles (ϕ_m). Therefore, clearly the problem in hand is to efficiently and jointly estimate these unknown parameters for $m = 1, 2, 3, \ldots, M$.

3. Proposed methodology

In this section, we have developed the hybrid PSO-PS scheme for the joint estimation of amplitude, frequency and the 2D DOA of plane waves (far field sources). The brief introduction, flow charts and parameters settings of PSO and PS are provided below.

3.1. Particle swarm optimization

Particle swarm optimization (PSO) is a global optimization method which was first proposed by Kennedy and Eberhart.[14] It is computationally less expensive than GA as it does not require cross over, mutation, elitism etc.[15] It is highly stochastic in nature and is a gradient-free algorithm. It can be used for noisy, linear, non-linear, differentiable and non-differentiable data. It has got applications in the diverse fields of science and engineering e.g., reactive power and control parameters,[16,17] the design of power system stabilizers,[18] short-range load forecasting,[19] chaotic systems[20] and Lorenz systems,[21] etc. In this current work, initially we have used PSO independently and then to improve the results further, it is hybridized with a local search optimizer called PS. The generic flow diagram of hybrid PSO is shown in Fig. 2, while its steps in the form of pseudo code are given below.

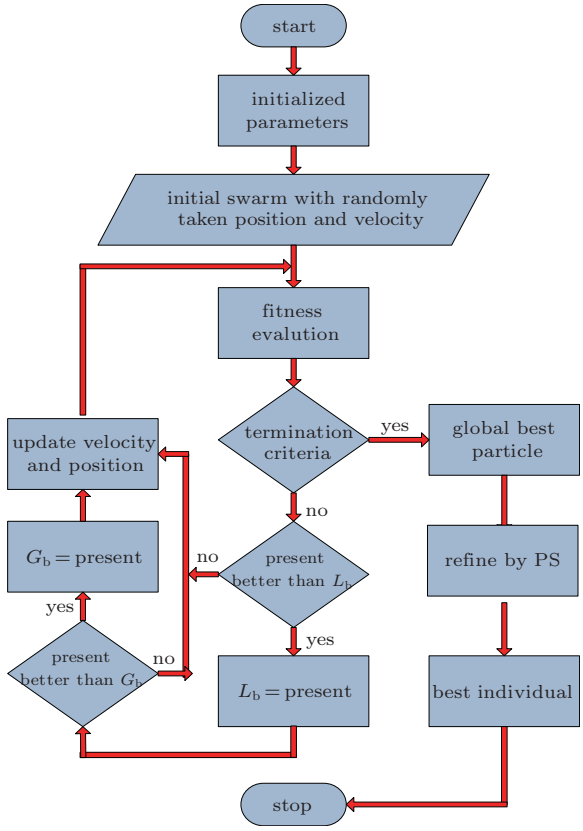


Fig. 2. (color online) Generic flow chart for PSO-PS technique.

Step I Initialization In this step, the swarm is randomly initialized and P particles are randomly generated. The length of each particle is $4 \times M$, where M is the number of far field sources. It can be given as

$$\begin{bmatrix} \boldsymbol{e}_1 \\ \boldsymbol{e}_2 \\ \boldsymbol{e}_3 \\ \vdots \\ \boldsymbol{e}_P \end{bmatrix} = \begin{bmatrix} s_{1,1}, s_{1,2}, \ldots, s_{1,M}, f_{1,M+1}, f_{1,M+2}, \ldots, f_{1,2M}, \theta_{1,2M+1}, \theta_{1,2M+2}, \ldots, \theta_{1,3M}, \phi_{1,3M+1}, \phi_{1,3M+2}, \ldots, \phi_{1,4M} \\ s_{2,1}, s_{2,2}, \ldots, s_{2,M}, f_{2,M+1}, f_{2,M+2}, \ldots, f_{2,2M}, \theta_{2,2M+1}, \theta_{2,2M+2}, \ldots, \theta_{2,3M}, \phi_{2,3M+1}, \phi_{2,3M+2}, \ldots, \phi_{2,4M} \\ s_{3,1}, s_{3,2}, \ldots, s_{3,M}, f_{3,M+1}, f_{3,M+2}, \ldots, f_{3,2M}, \theta_{3,2M+1}, \theta_{3,2M+2}, \ldots, \theta_{3,3M}, \phi_{3,3M+1}, \phi_{3,3M+2}, \ldots, \phi_{3,4M} \\ \vdots \\ s_{P,1}, s_{P,2}, \ldots, s_{P,M}, f_{P,M+1}, f_{P,M+2}, \ldots, f_{P,2M}, \theta_{P,2M+1}, \theta_{P,2M+2}, \ldots, \theta_{P,3M}, \phi_{P,3M+1}, \phi_{P,3M+2}, \ldots, \phi_{P,4M} \end{bmatrix}.$$

The above matrix can be represented as

$$\boldsymbol{E} = [\boldsymbol{e}_1, \boldsymbol{e}_2, \boldsymbol{e}_3, \ldots, \boldsymbol{e}_P]^{\mathrm{T}}. \tag{19}$$

The lower and upper bounds of s, f, θ, ϕ are defined as

$$\begin{aligned} &s_{p,m} \in R : l_b \le s_{p,m} \le u_b, \\ &f_{p,M+m} \in R : l_r \le f_{\min,M+m} \le f_{\max}, \\ &\theta_{p,2M+m} \in R : 0 \le \theta_{q,2M+m} \le \pi/2, \\ &\phi_{p,3M+m} \in R : 0 \le \phi_{q,3M+m} \le 2\pi, \end{aligned}$$

for $p = 1, 2, \ldots, P$ and $m = 1, 2, \ldots, M$, where l_b and u_b are the lower and upper bounds of amplitudes while $f_{\min}$ and $f_{\max}$ are the lower and upper ranges of frequencies.

Step II Fitness function (FF) We have used a new multi-objective fitness function. For the p-th particle, it can be expressed as

$$\mathrm{FF}(p) = \frac{1}{1 + \mathrm{err}(p)}, \tag{20}$$

where

$$\mathrm{err}(p) = \frac{1}{3Q}(\mathrm{err}_1(p) + \mathrm{err}_2(p) + \mathrm{err}_3(p)), \tag{21}$$

$$\mathrm{err}_1 = \left| y_{zq} - \hat{\boldsymbol{y}}_{zq}^p \right|^2 + \left| \left| \boldsymbol{y}_{zN}^H . \hat{\boldsymbol{y}}_{zN}^p \right| - 1 \right|, \tag{22}$$

where y_{zq} is defined in Eq. (1), while $\hat{y}_{zq}^p$ is defined as

$$\hat{\boldsymbol{y}}_{zq}^p = \sum_{m=1}^{M} \hat{e}_m \exp\left[-\mathrm{j} \frac{\hat{e}_{M+m}}{f_{\max}} (q\pi \cos(\hat{e}_{2M+m})) \right], \tag{23}$$

where $p = 1, 2, \ldots, P$. Similarly,

$$\mathrm{err}_2 = \left| y_{xq} - \hat{\boldsymbol{y}}_{xq}^p \right|^2 + \left| \left| \boldsymbol{y}_{xN}^H . \hat{\boldsymbol{y}}_{xN}^p \right| - 1 \right|, \tag{24}$$

where y_{xq} is defined in Eq. (14) while $\hat{y}^p_{xq}$ is defined as

$$\hat{y}^p_{xq} = \sum_{m=1}^{M} \hat{e}_m \exp\left[-\mathrm{j}\frac{\hat{e}_{M+m}}{f_{\max}}(q\pi \sin(\hat{e}_{2M+m}) \times \cos(\hat{e}_{3M+m}))\right] \tag{25}$$

and

$$\mathrm{err}_3 = \left|y_{yq} - \hat{\boldsymbol{y}}^p_{yq}\right|^2 + \left|\left|\mathbf{y}^H_{yN} \cdot \hat{\boldsymbol{y}}^p_{yN}\right| - 1\right|, \tag{26}$$

where y_{yq} is defined in Eq. (16) while, $\hat{y}_{yq}$ is defined as

$$\hat{\boldsymbol{y}}_{yq} = \sum_{m=1}^{M} \hat{e}_m \exp\left[-\mathrm{j}\frac{\hat{e}_{M+m}}{f_{\max}}(q\pi \sin(\hat{e}_{2M+m}) \times \sin(\hat{e}_{3M+m}))\right]. \tag{27}$$

In Eqs. (22), (24), and (26),

$$y_{wN} = \frac{\boldsymbol{y}_w}{\|\boldsymbol{y}_w\|}, \tag{28}$$

$$\hat{y}^p_{yN} = \frac{\hat{\boldsymbol{y}}_w}{\|\hat{\boldsymbol{y}}_w\|}, \tag{29}$$

where $w = x, y, z$. In this step, store each particle as a local best ($\boldsymbol{l}_{\mathrm{be}}$) and the one with maximum fitness function be stored as a global best ($\boldsymbol{g}_{\mathrm{be}}$).

Step III Termination criteria Terminate if any of the following conditions is satisfied, else go to step (IVa).

(i) The required error is achieved which is 10^{-10}.

(ii) The desired values of amplitude, frequency, elevation, and azimuth angles are attained.

Step IVa Update particle velocity The following relation is used to update the velocity of each particle

$$\boldsymbol{v}^n_p = \boldsymbol{v}^{n-1}_p + c_1 \mathrm{rand}_1(\boldsymbol{l}^{n-1}_{\mathrm{be}\,p} - \boldsymbol{e}^{n-1}_p) + c_2 \mathrm{rand}_2(\boldsymbol{g}^{n-1}_{\mathrm{be}\,p} - \boldsymbol{e}^{n-1}_p). \tag{30}$$

In the above equation, $\boldsymbol{v}^n_p$ represents the velocity of the p-th particle at flight n. The c_1 and c_2 are called the stochastic acceleration or self-confidence whose functions are to pull each particle towards global best and local best particles. For the ongoing problem $c_1 = c_2 = 1$. The rand_1 and rand_2 are two randomly generated vectors in the range $[0, 1]$. The velocity of each particle is doubly bounded as

$$-v_{\max} \le v_p \le v_{\max},$$

$$\text{if} \quad v_p(n) > v_{\max}, \quad v_p(n) = v_{\max},$$

$$\text{if} \quad v_p(n) < -v_{\max}, \quad v_p(n) = -v_{\max}.$$

Step IVb Update particle position To update the position of each particle, the following relation is used:

$$e_p(n) = e_p(n-1) + v_p(n). \tag{31}$$

Step Va Replace the local best particle Replace the previous local best particle with the new local best particle if the fitness of the new local best particle is better than the previous one.

Step Vb Replace the global best particle Similarly replace the previous global best particle with the new one if the fitness of the new one is better than the old one.

Step VI Hybridization Once the best possible results are achieved by PSO alone, give them as a starting point to PS to make them even better. The PS is discussed in the subsequent sub-section.

Step VII Storage Store all the results of PSO and hybridized PSO for comparison and analysis.

3.2. Pattern search technique

The idea of PS, was first given by Hookes and Jeeves.[22] The main purpose of PS is to compute a chain of points in order to reach an optimal point. In every step, the PS attempts to find a mesh (set of points) around the optimal point of previous step. One can achieve the mesh by adding the existing point to a scalar multiple of vectors called a pattern.[23] In the next step of the algorithm, the new point takes the position of the current point provided the technique locates the point in the mesh that improves the objective function of the current point. In order to get the optimum value of the objective function, the PS technique is repeated again and again until any of the following conditions are achieved:

(i) The size of mesh becomes less than its tolerance.

(ii) The gap between successful and subsequent successful poles is lower than the set tolerance.

(iii) The total number of iterations has reached a predefined value.

It can be used as global optimizer, as well as a local search optimizer but its performance is better when it is used as local optimizer with any other global optimization method.[24–26]

Table 1. Parameter setting for PS.

Parameters	Setting
Starting point	the best particle achieved through PSO
Poll method	GPS positive basis
Polling order	consecutive
Maximum iteration	3000
Function evaluation	15000
Mesh size	01
Expansion factor	2.0
Contraction factor	0.5
Penalty factor	100
Bind tolerance	10^7
Mesh tolerance	10^{10}
X tolerance	10^{10}

For PS, we have used a MATLAB built-in optimization tool box for which the parameter settings are given in Table 1, while its generic flow diagram is shown in Fig. 3.

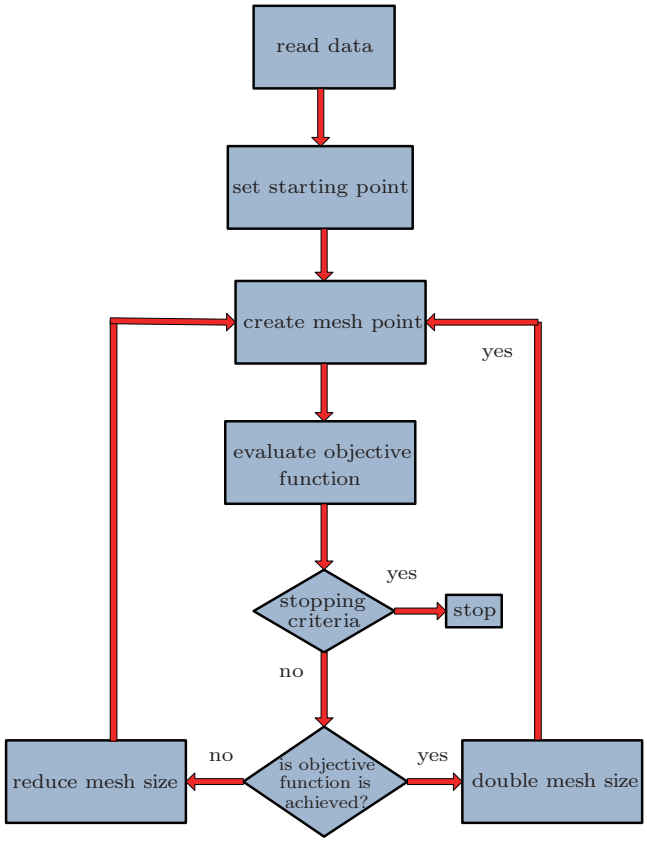


Fig. 3. (color online) Generic flow chart for pattern search technique.

4. Results and discussion

In this section, we have carried out several simulations to assess the performance of the proposed (PSOPS) scheme. This section is mainly divided into two parts. In the first part, the estimation accuracy, convergence rate, proximity effect and performance on the reference axis of the proposed hybrid scheme is evaluated. The results are not only compared with PSO and PS alone but also with the other hybrid GAPS technique discussed in Ref. [12]. In the second part, the proposed scheme is compared with a non-heuristic traditional technique[13] using an error as a figure of merit. Throughout the simulation, a single snapshot is used, while the value of $f_{\max}$ is taken to be 90 MHZ. All the values of DOA and the frequencies are taken in radians (rad) and Hertz (Hz), respectively and each result is averaged over 100 independent trials.

4.1. Comparison of PSO-PS with PSO, PS and GA-PS

In this subsection, we have compared PSO-PS with PSO, PS and GA-PS in terms of estimation accuracy, convergence rate and proximity effect. In Ref. [12], a hybrid scheme (GA-PS) using 2-L shaped array is developed for the joint estimation of amplitude, elevation and azimuth angles using MSE as a fitness evaluation function. Reference [12] has shown better performance than that of GA alone and the propagator method.[9,10] Hence, we will compare our results only with that of GA-PS. Moreover, reference [12] has not discussed the frequency estimation, so the comparison of the proposed approach is done with the amplitude, elevation and azimuth angles only.

4.1.1. Estimation accuracy

In this sub-section, two cases are considered based on the number of sources. No noise is added to the system.

Case 4.1.1a In this case, three sources are taken which have the desired values of amplitude, frequency, elevation and azimuth angles: $s_1 = 1$, $f_1 = 80$ MHz, $\theta_1 = 1.0472$ rad, $\phi_1 = 3.8397$ rad, $s_2 = 4$, $f_2 = 55$ MHz, $\theta_2 = 0.5236$ rad, $\phi_2 = 1.6581$ rad, $s_3 = 7$, $f_3 = 70$ MHz, $\theta_3 = 0.7854$ rad, $\phi_3 = 2.1817$ rad. The 2-L shaped array consists of seven sensors i.e., each ULA is composed of two sensors whereas the reference sensor is common for them. As listed in Table 2, one can observe the advantage of the hybridization of a global optimizer with a local search optimizer. The PSO alone is less accurate than GA-PS but when we hybridized PSO with PS, it produced even better results than GA-PS. Therefore, in this case, the proposed PSO-PS technique proved to be the most accurate scheme.

Table 2. Estimation accuracy for three sources.

Scheme	s_1	f_1/MHz	θ_1/rad	ϕ_1/rad	s_2	f_2/MHz	θ_2/rad	ϕ_2/rad	s_3	f_3/MHz	θ_3/rad	ϕ_3/rad
Desired	1.0000	80.0000	1.0472	3.8397	4.0000	55.0000	0.5236	1.6581	7.0000	70.0000	0.7854	2.1817
PS	1.6087	77.9810	1.099	3.8990	3.5812	53.3807	0.5825	1.6971	7.7189	72.0195	0.7466	2.1127
PSO	1.0034	80.0037	1.0629	3.8361	4.0035	54.9963	0.5271	1.6619	6.9965	69.9960	0.7888	2.1852
GA-PS	0.9996	–	1.0664	3.8393	4.0004	–	0.5240	1.6585	6.9997	–	0.7858	2.1813
PSO-PS	1.0000	80.0001	1.0473	3.8397	4.0000	55.0002	0.5236	1.6582	7.0000	70.0001	0.7855	2.1817

Case 4.1.1b In this case, four far field sources are taken which have the desired values given below. $s_1 = 5$, $f_1 = 40$ MHz, $\theta_1 = 0.4363$ rad, $\phi_1 = 1.9199$ rad, $s_2 = 3$, $f_2 = 50$ MHz, $\theta_2 = 0.8772$ rad, $\phi_2 = 2.4435$ rad, $s_3 = 8$, $f_3 = 60$ MHz, $\theta_3 = 1.1345$ rad, $\phi_3 = 0.6981$ rad, $s_4 = 2$, $f_4 = 45$ MHz, $\theta_4 = 0.2618$ rad, $\phi_4 = 2.6180$ rad.

Table 3. Estimation accuracy for four sources.

Scheme	s_1	f_1/MHz	θ_1/rad	ϕ_1/rad	s_2	f_2/MHz	θ_2/rad	ϕ_2/rad
Desired	5.0000	40.0000	0.4363	1.9199	3.0000	50.0000	0.8720	2.4435
PS	3.9688	44.0316	0.3050	1.7879	2.4689	45.9684	0.9233	2.3121
PSO	5.0091	40.0094	0.4271	1.9282	3.0094	49.9905	0.8630	2.4522
GA-PS	5.0040	–	0.4404	1.9231	3.0042	–	0.8679	2.4476
PSO-PS	4.9983	39.9980	0.5381	1.9208	2.9282	49.9979	0.8739	2.4416
Scheme	s_3	f_3/MHz	θ_3/rad	ϕ_3/rad	s_4	f_4/MHz	θ_4/rad	ϕ_4/rad
Desired	8.0000	60.0000	1.1345	0.6981	2.0000	45.0000	0.2618	2.6180
PS	8.5316	64.0317	1.4031	0.6167	1.4689	49.0318	0.2106	2.6994
PSO	8.0095	59.9903	1.1436	0.6889	2.0094	45.0097	0.2526	2.6090
GA-PS	8.0043	–	1.1305	0.6940	2.0043	–	0.2577	2.6261
PSO-PS	8.0020	60.0022	1.1364	0.6997	1.9982	39.9978	0.2601	2.6164

Due to the increase of unknowns, the performance of PSO and PS alone are spoiled a lot, as we have faced few local minima in this case. However, the hybrid schemes, especially the PSO-PS, produced fairly good estimation accuracy even in this case. The second best scheme is GA-PS as given in Table 3.

4.1.2. Convergence rate

In this sub-section, we have performed simulations to check the convergence rate of our proposed hybrid scheme. For convergence we mean the total number of times a particular algorithm achieved its desired goal, out of the total number of trials. This experiment is done in the presence of 10 dB noise and the array consists of ten sensors. As shown in the bar graph of Fig. 4, the hybrid PSO-PS scheme converges for the most number of times as compared to the other schemes for all numbers of sources. The PSO-PS scheme converged 98%, 95% and 93% for two, three and four sources, respectively. The second best scheme is the other hybrid GA-PS scheme. The convergence rate is degraded for each scheme with the increase of sources.

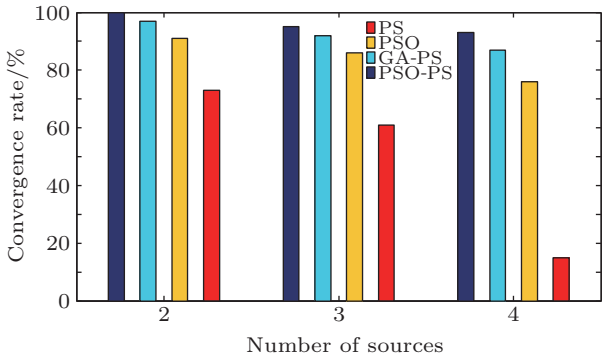


Fig. 4. (color online) Convergence rate versus the number of sources for 2-L shaped array at 10 dB noise.

4.1.3. Proximity effect

In this simulation, we have checked the proposed scheme for the sources located close to each other. In this experiment, the PSO-PS is only compared with GA-PS of Ref. [12]. For this simulation, the 2-L shaped array consists of ten sensors and 10 dB noise is added. In Table 4, first the proximity of the elevation angles are checked and then the proximity of the azimuth angles are provided for fixed values of amplitudes and frequencies. The estimation accuracy, as well as the convergence rate, of both hybrid schemes is degraded when the elevation and azimuth angles are brought close to each other. This degradation is quite obvious as we have faced few strong local minima. However, again one can see that both hybrid schemes have produced fairly good results. However, the PSO-PS scheme is more effective as compared with GA-PS even in this case.

Table 4. Proximity effect of elevation and azimuth angles at 10 dB noise.

Scheme	θ_1/rad	θ_2/rad	θ_3/rad	ϕ_1/rad	ϕ_2/rad	ϕ_3/rad	Convergence rate/%
Desired	0.4363	0.6981	1.0472	2.0944	2.7925	1.3963	–
GA-PS	0.0467	0.6977	1.0477	2.0948	2.7921	1.3967	97
PSO-PS	0.0462	0.6981	1.0471	2.0944	2.7926	1.3962	100
Desired	0.4363	0.5236	1.0472	2.0944	2.7925	1.3963	–
GA-PS	0.4389	0.5209	1.0477	2.0948	2.7921	1.3967	91
PSO-PS	0.4372	0.5251	1.0471	2.0944	2.7926	1.3962	97
Desired	0.4363	0.5236	0.6109	2.0944	2.7925	1.3963	–
GA-PS	0.4332	0.5268	0.6141	2.0948	2.7921	1.3967	81
PSO-PS	0.4346	0.5252	0.6125	2.0944	2.7926	1.3962	90
Desired	0.4363	0.6981	1.0472	2.0944	2.1817	1.3963	–
GA-PS	0.0467	0.6977	1.0477	2.0973	2.1847	1.3967	90
PSO-PS	0.0462	0.6981	1.0471	2.0929	2.1831	1.3962	97
Desired	0.4363	0.6981	1.0472	2.0944	2.1817	2.2689	–
GA-PS	0.0467	0.6977	1.0477	2.0901	2.1859	2.2649	80
PSO-PS	0.0462	0.6981	1.0471	2.0926	2.1835	2.2671	90

Case 4.1.4 Performance on reference axis

In this sub-section, the proposed scheme is checked for more the practical scenario where the DOA of the sources is taken on the reference axis. For this purpose, the 2-L shaped array is composed of 13 sensors and four sources are considered which have desired values of $s_1 = 2$, $f_1 = 40$ MHz, $\theta_1 = 0$ rad, $\phi_1 = 1.5708$ rad, $s_2 = 5$, $f_2 = 50$ MHz, $\theta_2 = 1.5708$ rad, $\phi_2 = 0$ rad, $s_3 = 1$, $f_3 = 60$ MHz, $\theta_3 = 1.2217$ rad, $\phi_3 = 3.1416$ rad, $s_4 = 4$, $f_4 = 70$MHz, $\theta_4 = 1.0472$ rad, $\phi_4 = 4.7124$ rad.

As provided in Table 5, the estimation accuracy of both hybrid schemes despoiled for the elevation angles on the reference axis and produced significant errors.

Table 5. Performance on the reference axis.

Scheme	θ_1/rad	ϕ_1/rad	θ_2/rad	ϕ_2/rad	θ_3/rad	ϕ_3/rad	θ_4/rad	ϕ_4/rad
Desired	0.0000	1.5708	1.5708	0.0000	1.2217	3.1416	1.0472	4.7124
GA-PS	0.1065	1.5832	1.4653	0.0375	1.2300	3.1486	1.0555	4.7195
PSO-PS	0.1040	1.5757	1.6748	0.0165	1.2245	3.1446	1.0491	4.7152

However, one can deduce that the PSO-PS scheme is less affected as compared with GA-PS. On the other hand, the azimuth angles on the reference axis have produced negligibly small error especially in the case of the PSO-PS technique.

5. Comparison with a traditional non-heuristic technique[13]

In Ref. [13] a hierarchical space-time decomposition method is used for the joint estimation of frequencies and 2D DOA of far field sources impinging on a uniform rectangular array (URA). It basically makes use of the 1D ESPRIT algorithm along with MSE as a cost function. We have compared the error achieved by our proposed scheme (using Eq. (22)) to the MSE of Ref. [13]. As Ref. [13] has not estimated the amplitudes, therefore, we will not consider it in this section. For this experiment, we have considered the same two cases, with the same values of frequencies, elevation and azimuth angles as discussed in Section 4.1. The 2-L shaped array and URA are composed of 13 and 36 sensors respectively. The values of signal to noise ratio (SNR) range from -5 dB to 25 dB. As shown in Figs. 5–7, the proposed scheme maintained a minimum error for frequencies, elevation angles and azimuth angles in both cases as compared to Ref. [13] for all values of SNR. More importantly, our proposed scheme utilized fewer sensors as compared with Ref. [13] and thus requires a smaller hardware budget to implement.

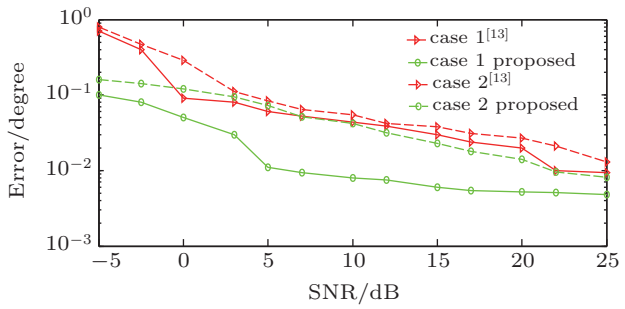


Fig. 5. (color online) Comparison of the frequency estimates.

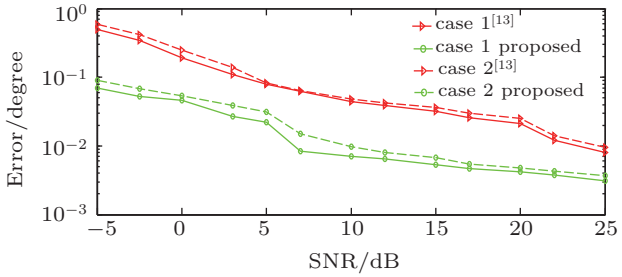


Fig. 6. (color online) Comparison of the elevation estimates.

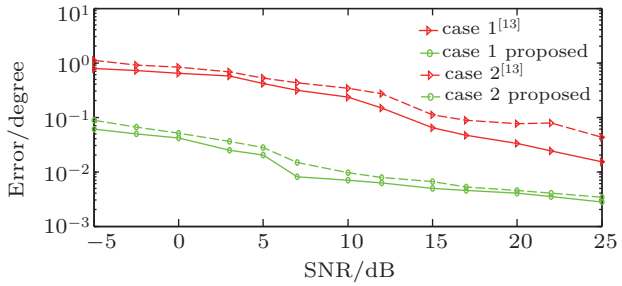


Fig. 7. (color online) Comparison of the azimuth estimates.

6. Conclusion and future work

In this work, a hybrid PSO-PS technique is developed for the joint estimation of the amplitude, frequency and 2D DOA of plane waves impinging on a 2-L shaped array. It has used a new multi-objective fitness function which is the combination of MSE and the correlation of normalized desired and estimated vectors. It has been noticed that the performance, especially in terms of robustness, is not up to the mark when PSO is used in an actual case i.e., independently. However, PSO has produced better robustness against noise when it is hybridized with PS. Over all, the proposed scheme has shown better results as compared with those of PSO, PS and GA-PS in terms of estimation accuracy, robustness, convergence rate and proximity effect. It has also shown better results as compared with the traditional approach in terms of error and number of sensors. In future, one can see the proposed scheme for side lobe

reduction, null steering and beam steering in the field of adaptive beamforming.

References

[1] Krim H and Viberg M 1996 *IEEE Signal Process. Mag.* **4** 67
[2] Bencheikh M L and Wang Y 2011 *Prog. Electromagn. Res. Lett.* **22** 109
[3] Byrne D, Halloran M O, Glavin M and Jones E 2010 *Prog. Electromagn. Res.* **107** 331
[4] Nishiura T and Nakamura S 2003 *IEEE Workshop on Statistical Signal Processing*, September 28–October 1, 2003, Missicipe, p. 597
[5] Xiong H, Hong J S and Zhu Q Y 2012 *Chin. Phys. Lett.* **29** 114102
[6] Jin D L, Hong J S and Xiong H 2012 *Chin. Phys. Lett.* **29** 104101
[7] Sotiriou A I, Varlamos P K, Trakadas P and Capsalis C N 2006 *Prog. Electromagn. Res.* **62** 89
[8] Liu T H and Mendel J M 1998 *IEEE Trans. Signal Process.* **46** 2061
[9] Marcos S 1993 *J. Acoust. Soc. Am.* **93** 1978
[10] Hua T K S and Weiner Y D 1991 *IEEE Antennas Propag. Mag.* **39** 143
[11] Tayem N and Kwon H M 2005 *IEEE Antennas Propag. Mag.* **53** 1622
[12] Zaman F, Qureshi I M, Khan J A and Khan Z U 2013 *Int. J. Antennas Propag.* **2013** 593247
[13] Lin C H, Fang W H, Lin J D and Wu K H 2010 *Signal Process.* **1** 207
[14] Kennedy J and Eberhart R C 1995 *IEEE International Conference on Neural Networks*, October 3–5, 1995, Perth, Australlia, p. 1942
[15] Yoshida H, Kawata K, Fukuyama Y, Takayama S and Nakanishi Y 2000 *IEEE Trans. Power Syst.* **15** 1232
[16] Zhao B, Guo C X and Cao Y J 2005 *IEEE Trans. Power Syst.* **20** 1070
[17] Fang W, Sun J, Xie Z P and Xu W B 2010 *Acta Phys. Sin.* **59** 3686 (in Chinese)
[18] Huang C M, Huang C J and Wang M L 2005 *IEEE Trans. Power Syst.* **20** 1126
[19] Gaing Z L 2003 *IEEE Trans. Power Syst.* **18** 1187
[20] Gao F and Tong H Q 2006 *Acta Phys. Sin.* **55** 577 (in Chinese)
[21] Li Z Q, Tong H Q and Gao F 2008 *Chin. Phys. B* **17** 1196
[22] Hooke R and Jeeves T A 1961 *J. ACM (JACM)* **8** 212
[23] Torczon V 1997 *SIAM J. Optim.* **1** 1
[24] Zaman F, Qureshi I M, Naveed A, Khan J A and Asif Z R M 2012 *Prog. Electromagn. Res. B* **39** 319
[25] Zaman F, Khan J A, Khan Z U and Qureshi I M 2013 *IEEE Conference Applied Sciences and Technology (IBCAST)*, January 04–06, 2013, p. 364
[26] Khan S U, Qureshi I M, Zaman F and Naveed A 2013 *Prog. Electromagn. Res. B* **52** 165